

A HEAT SINK THERMAL DESIGN FOR THE SSC PASSIVE QUENCH PROTECTION DIODES

Ruben H. Carcagno
SSC CENTRAL DESIGN GROUP

December 1987

SUMMARY

During an SSC quench, a bypass diode (initially at 4.35 K) will be subject to a current pulse of 6500 A max. with an exponential decay of 20 sec of time constant. The power generated at the diode junction during the current flow ($P = I \cdot VF$, I: current, VF: forward voltage drop) has to be dissipated in order to maintain the junction temperature below 170 C (this temperature is a limit specified by the manufacturer). The present solution is to use the diode holder device also as a heat sink, with Copper blocks of adequate dimensions.

In this note we present a thermal design for the heat sink of the passive quench protection diodes. These diodes are subject to unusual operating conditions in the SSC: thermal cycling between 4.35 K and above room temperature in most cases, and degradation of its operating characteristics due to radiation exposure. Therefore, it is not possible to use conventional recipes and criteria for heat sink thermal design under this unusual operating conditions.

From the heat sink thermal design point of view, the main effect of the radiation exposure is an increase in VF, thus an increase in the power dissipated at the junction during an SSC quench current pulse. It is the heat sink that puts a limit in how much VF is allowed to increase for safe diode operation, because due to the transient nature of the quench pulse there is a forward voltage drop beyond which it is no longer possible to maintain the junction temperature below 170 C, no matter how large we make the heat sink. Therefore, the design criteria for the heat sink was to find a set of "optimum" dimensions such that the junction temperature was below 170 K for a reference SSC quench current pulse and for the maximum possible average forward voltage drop.

The thermal cycling between Liquid Helium temperatures and room temperature introduces strong non-linearities in the problem due to the materials properties dependence on temperature. We used the non-linear, time-dependent Finite Element program TOPAZ to solve the heat diffusion equation. Contact thermal resistances were studied (particularly at low temperatures), and included in the calculations.

As a result of our studies, we propose to specify a Copper heat sink of at least 5 cm radius and 4 cm thick at both sides of the diode package. This heat sink should be enough to limit the maximum junction temperature below 170 C for an irradiated diode with an average forward voltage drop of 2.3 V (produced by more than a 100 years of SSC operation according to present estimates) during an SSC quench pulse, even in the event of a failure of one dump resistor.

INTRODUCTION

The passive quench protection system being considered for the SSC requires power diodes at Liquid Helium temperature in order to increase the diode's "turn-on" voltage, thus avoiding current bypass while changing the current in the magnets. The present solution is to place the diodes in magnet cryostat, but as a consequence of their proximity to the beam line the diodes will be exposed to a neutron flux of approximately 3.2×10^{11} neutrons-cm² per SSC year according to present estimates /1/.

The diodes are required to survive to a quench current pulse of approximately 6500 Amps with an exponential decay of 20 sec time constant.

The main reason for power diodes catastrophic failure is junction temperature excess (> 170 C according to specifications /2/). Physical destruction of the device is caused by "burnout" of the Silicon wafer.

The junction temperature is determined by the combined effects of power dissipation at the junction ($P = I \cdot VF$) and heat diffusion through adjacent materials. The forward voltage drop VF for a given diode depends on current, temperature, and radiation damage. Radiation increases VF at a given current and temperature (in some cases the opposite is true, but this effect is not important at the levels we are considering), so we expect an increase in the maximum junction temperature during a quench current pulse with increasing radiation exposure. The heat sink is the limiting factor in the junction temperature increase, and the question of how much VF can increase and the junction temperature be still below 170 C is strongly related to the heat sink design. Furthermore, given the transient nature of the SSC quench current pulse, there is a maximum VF beyond which it is no longer possible to maintain the junction temperature below 170 C, no matter how large we make the heat sink. Therefore, the heat sink is strongly related to a "dose limit" criteria for the diodes. If the heat sink is designed right, its dimensions should not be a limiting factor for the maximum VF increase allowed for safe diode operation. The limiting factors will be the transient characteristics of the current pulse, the heat sink material, and the diode package - heat sink contact conditions.

Our aim was to design this "optimum" heat sink for the passive quench protection diodes. As a plus, we also obtained a maximum forward voltage drop for safe diode operation. This maximum value of VF can be related to measurements of VF as a function of neutron exposure /3/ to establish a "dose limit" criteria. However, we must point out that other dose limit criteria can emerge from studies of effects such as current crowding, self-annealing, positive temperature coefficients, "open" failure, etc. Nevertheless, failure because of maximum uniform temperature excess have to be considered in any dose limit criteria.

The diode that we considered for our analysis was the BBC diode DS6000, a strong candidate at the present moment due to its radiation hardness /3/. The heat sink is part of the diode holder device, and it consists of copper blocks pressed against the diode commercial package. We calculated the junction temperature by solving the heat diffusion equation in the diode package plus heat sink with the non-linear, time-dependent Finite Element code TOPAZ2D /4/. Strong non-linearities are introduced because of the materials properties dependence on temperature. Contact thermal resistances within the diode package and between the diode package and the heat sink have an important effect on the junction temperature. We have studied the problem, particularly at low temperatures (see Appendix D), and we have extrapolated several published values to our case. We included contact thermal resistances in our calculations.

The 20 sec decay constant of the quench current pulse is determined by the sector energy dissipation through 4 dump resistors of .28 ohms each (sector inductance: 22 H). In our calculation, we assumed that one dump resistor fails, what increases the time constant to 26 sec. Our "reference" SSC quench current pulse has a 300ms rise time up to 6500 Amps, and then an exponential decay with 26 sec time constant. Therefore, our heat sink thermal design has some safety margin in case of a dump resistor failure.

1. THE DIODE PACKAGE

The DS6000 diode comes in a presspack housing. Fig. 1 shows an example of a 3" presspack housing, and Fig. 2 shows a picture of the commercial package for the DS6000. Fig. 3 shows the dimensions of the DS6000 package. The Silicon chip is very thin (typically .14 mm), with a diameter of approximately 45 mm. At one side, the Si chip is alloyed to a 1 mm thick Molybdenum disk. At the other side, there is a .01 mm thick layer of Aluminium, a special lubricant, and a .1 mm Molybdenum disk. This latter configuration allows sliding of the Si chip with the thinner Molybdenum disk during thermal cycling with the minimum wear. The Molybdenum disk is thinner than the one alloyed at the other side to compensate for the contact thermal resistance of the sliding surface. Both Molybdenum disks are in contact with 34 mm thick nickel plated copper pole pieces. The electrical and thermal contact is established by a clamping force of 20,000 N applied to the outside of the housing.

Schematic construction of a 3" presspack housing. The alloyed silicon chip (1) is contacted on the cathode side by a pressure plate (2). (1) and (2) are contacted in the housing by 2 nickel plated copper pole pieces (3). All components are electrically and thermally contacted by an external clamping force. The external air gap and creepage path is provided by a glazed ceramic housing (4).

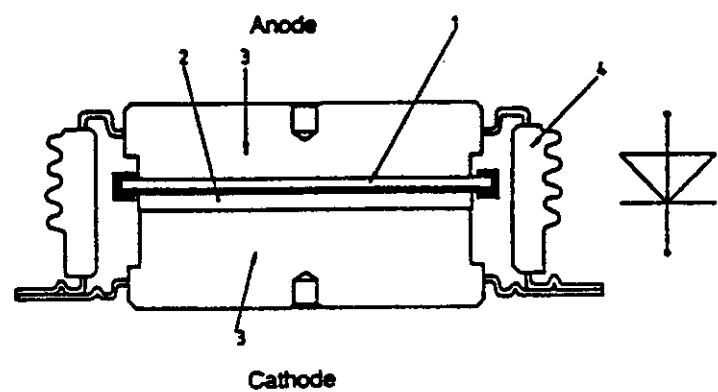
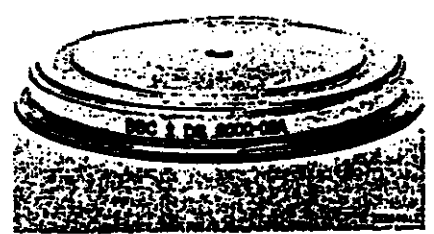


Fig. 1: Example of a diode package schematic construction.



Diode
DS 6000

$I_{FRMS} = 14200 \text{ A}$
 $I_{FAYM} = 6100 \text{ A}$
 $V_{RRM} = 200 \text{ V}$

Fig. 2: The DS6000 package.

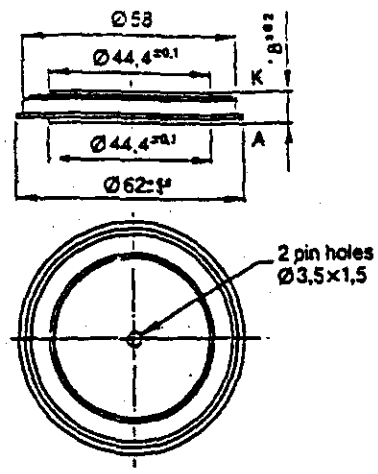


Fig. 3: DS6000 package dimension

2. THE MOUNTING ASSEMBLY

The diode package has to be hold in a mechanical device able to apply a clamping force of 20-24 kN according to specifications. The holder (mounting assembly) usually plays also the role of heat sink. There are two examples of mounting assembly devices for quench protection diodes: the Hera design (see Fig. 5) and the BNL design for Isabelle (see Fig. 6). In both cases provisions have been taken to absorb dimensional changes due to thermal expansions/contractions during thermal cycles. The best solution at the moment seems to be to apply the compressive force with Belville Washers made from Copper Beryllium (to prevent fracture at low temperature). At both end there are Stainless Steel caps for structural purposes. Once the heat sink (Copper blocks) is designed, the next logical step is to calculate thermal stresses and deformations of the mounting assembly during a thermal cycle. Structural analysis is necessary because we have to be sure that during the whole thermal cycle the clamping force remains within specifications (we have made this assumption for the heat sink thermal design). If this is not the case, then either the contact thermal resistances will increase (lower contact pressure) or the friction coefficient will increase (higher contact pressure). In both cases the result is going to be premature failure by either temperature excess or wearout.

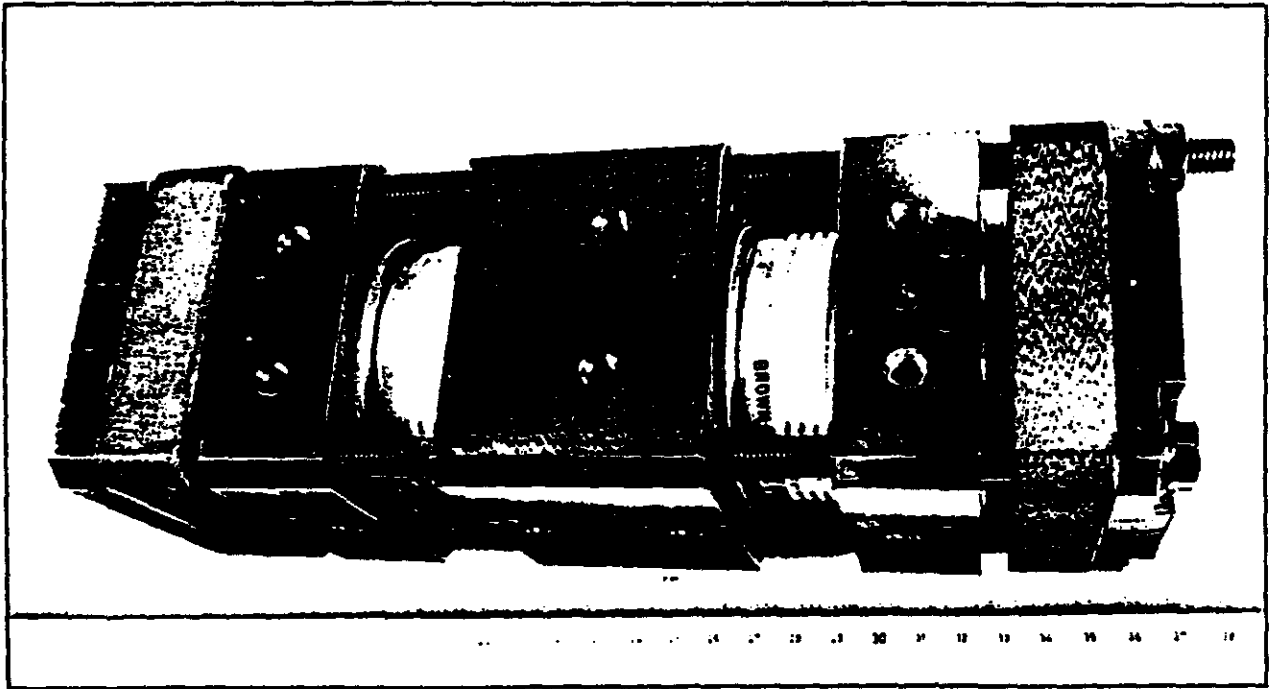


FOTO DESY, J.Schmidt, 40387/15 - 19.01.1987

Fig. 5: HERA mounting assembly design.

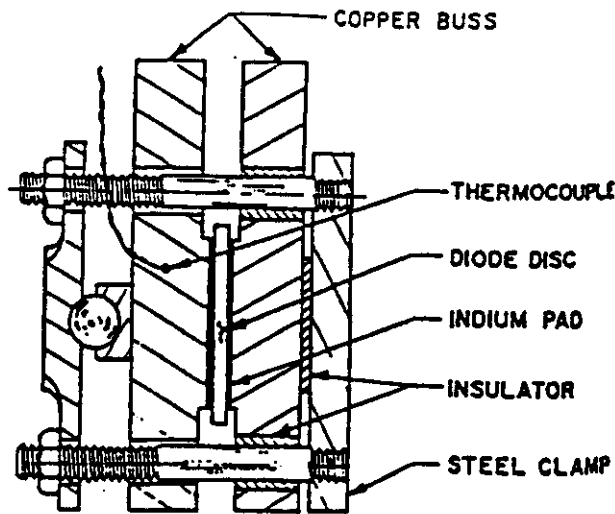


Fig. 6: BNL mounting assembly design (for Isabelle)

3. THE MODEL

3.1 Geometry

We considered a two-dimensional axysymmetric geometry. Although the Copper blocks are not cylinders, we made this approximation with the understanding that the cylinder has to be inscribed in the copper block, so this is a conservative assumption. We also considered thermal symmetry at both sides of the junction. We neglect the effect of the Stainless Steel end caps as heat sink. At least in the Belville Washers side, the thermal coupling is very weak (small contact area). This is also a conservative assumption.

Fig. 7 shows the geometry (and the Finite Element mesh for TOPAZ2D) for a heat sink with $R = 5$ cm and $L = 4$ cm.

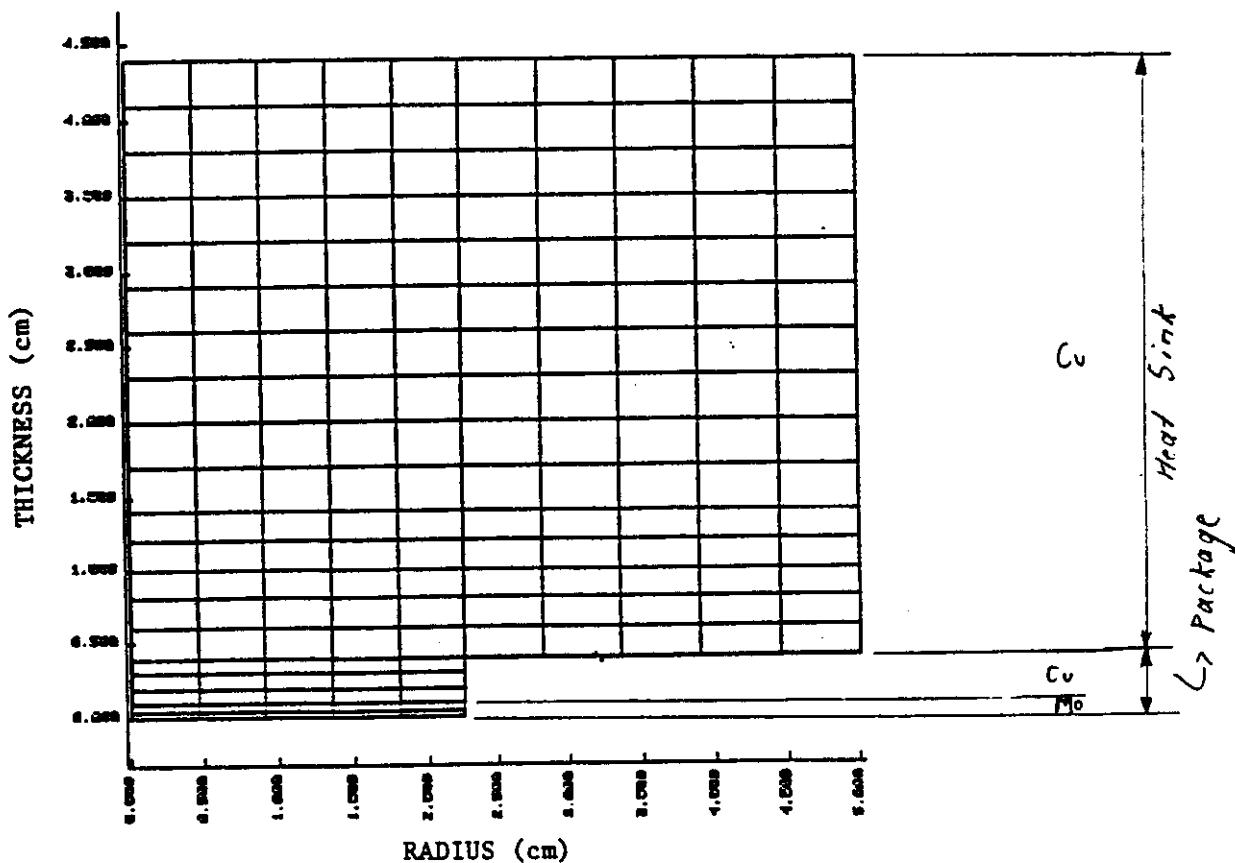
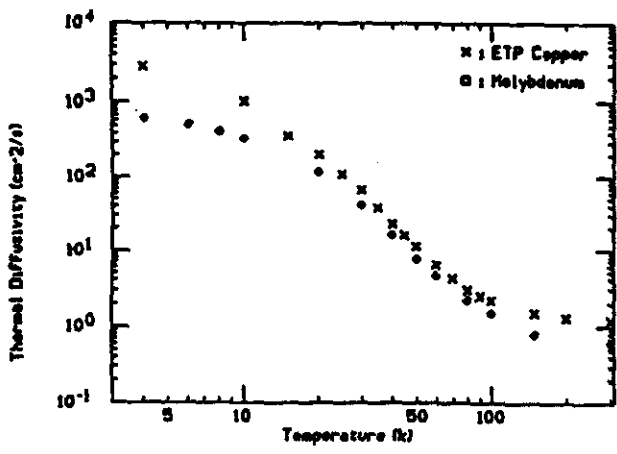
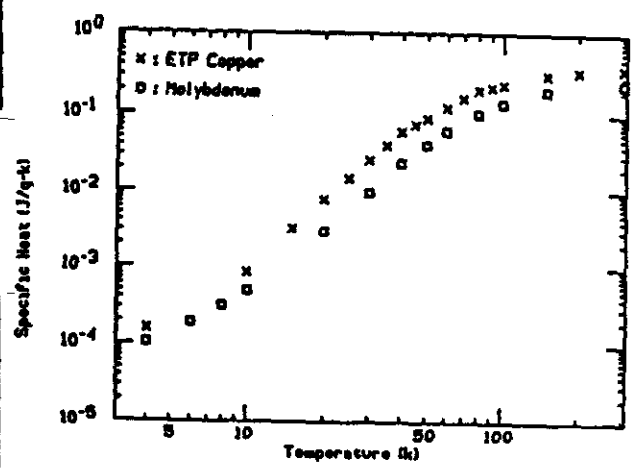
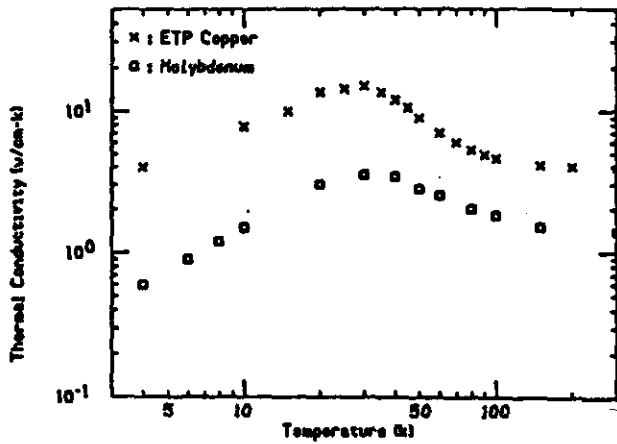


Fig. 7: Geometry and F.E. mesh

3.2 Materials

We considered two materials: Molybdenum and ETP Copper. All other (Silicon, Aluminium, Nickel, Stainless Steel) are not relevant from the thermal point of view. Silicon has a high thermal diffusivity compared to Molybdenum and Copper, and its thickness is very small for the diffusion times we are considering. Figs. 8 to 10 show values of thermal conductivity, specific heat and thermal diffusivity for Molybdenum and ETP copper as a function of temperature. Those are the properties we used in our simulations.

Figs. 8-10: Thermal Conductivity, Specific Heat, and Thermal Diffusivity as a function of temperature for ETP Copper and Molybdenum (from standard reference Handbooks).



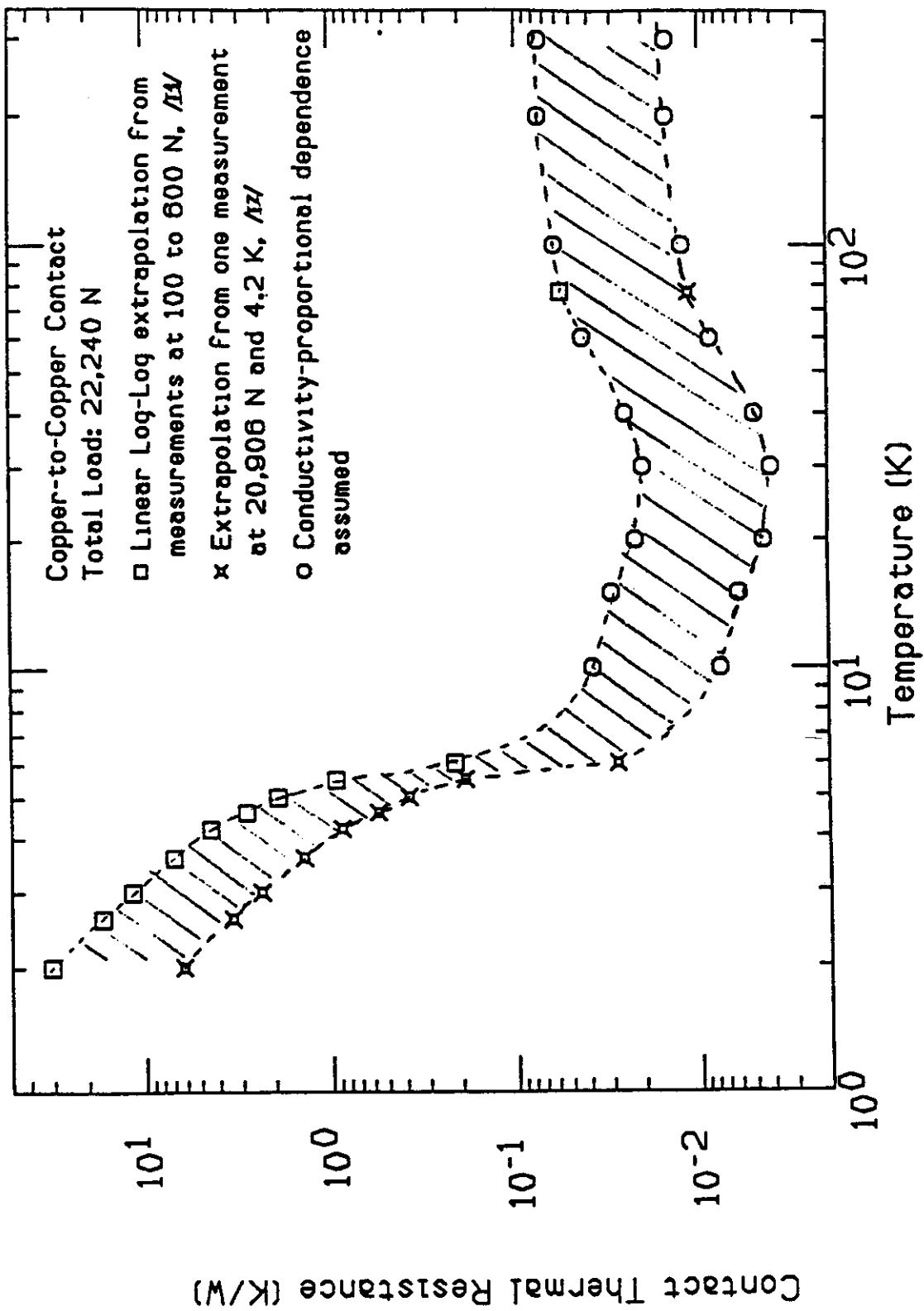


Fig. 11: Estimated contact thermal resistance between the diode package and the heat sink (see Appendix I)

3.3 Contact Thermal Resistance (CTR)

There are two CTRs to consider in our model: one inside the DS6000 package, between the Molybdenum disk and the Copper disk, and the other between the diode package and the heat sink. We consider the thick Molybdenum side, so there is no CTR between the Silicon chip and Molybdenum (they are alloyed).

The question was which is the CTR behavior at low temperatures. We found several publications of experimental work in metal-to-metal CTR in vacuum as a function of applied contact forces, surface finishing, temperature, and heat flux. The specimen pairs under study were mainly Copper, Stainless Steel, and Aluminium. Unfortunately, most of the measurements were done at a lower contact force, so we had to extrapolate those measured values to our conditions. Fig. 11 shows our estimated range of CTR between the diode package and the heat sink as a function of temperature. Appendix I explains how this CTR was estimated. Qualitatively, we can say that a dramatic increase in the CTR occurs below ~ 10 K, with a $1/T^2$ dependence. For our thermal analysis, we can assume that above 10 K the CTR remains approximately constant, and equal to its room temperature value.

The CTR inside the diode package was estimated in the following way: As part of the DS6000 specifications, the junction-case thermal resistance is 0.02 K/W (one side cooling). This thermal resistance includes materials thermal resistances due to conductivity ($R = L/KA$, where L is the thickness, K the conductivity and A the area) plus the contact thermal resistance. The thermal resistance of the Silicon, Molybdenum and Copper disks inside the diode package is about 0.01 K/W (at room temperature). The remaining 0.01 K/W is the contact thermal resistance between the Molybdenum disk and the Copper disk.

The Contact thermal resistance between the case and the heat sink is also specified: 0.01 K/W. However, if the diodes are placed in a vacuum environment we expect this CTR to increase because heat transfer through the interstitial medium can be neglected (see Appendix I). We decided to use a CTR of 0.02 K/W between the diode package and the heat sink, which is a representative value in the range 10 K - 300 K according to our estimates (see Fig. 11). Uncertainties in the CTR values are by far the major source of error in our calculations.

In summary, we used the following CTR values:

Molybdenum - Copper CTR = 0.01 K/W

Diode package - Heat sink = 0.02 K/W

3.4 The diode forward voltage drop (VF)

For a given diode, VF depends on current, temperature, and radiation damage. Fig. 12 shows the approximate dependence of the DS6000 VF on current and temperature for an undamaged diode (there are a few measured points in that curves, that have to be regarded as an estimation of the VF behavior with temperature and current. We are planning to take more measurements in the near future). Below ~ 30 K there is a dramatic increase in VF. It is this characteristic what makes cold diodes so attractive for passive quench protection; a switch-like behavior activated by a high enough forward voltage. After ~ 30 K, the diode is back into its "normal" characteristic of low forward voltage drop. Nevertheless, the diode still shows a negative temperature coefficient all the way up to high temperatures, but this

(almost constant) negative temperature coefficient is much smaller in magnitude than the one below ~ 30 K.

The VF dependence in current is relatively small compared to its dependence on temperature. Radiation damage can not only change the voltage scale in Fig. 12, but also its shape. For the Westinghouse RA20, for example, we found that after a certain amount of radiation exposure the diode showed a positive temperature coefficient at high temperatures. We haven't seen evidence of this radiation-induced positive temperature coefficient for the DS6000, but in the next reactor run we are planning confirm this observation through measurements of VF as a function of temperature for an irradiated diode. Annealing and self-annealing effects also contribute to the change in shape.

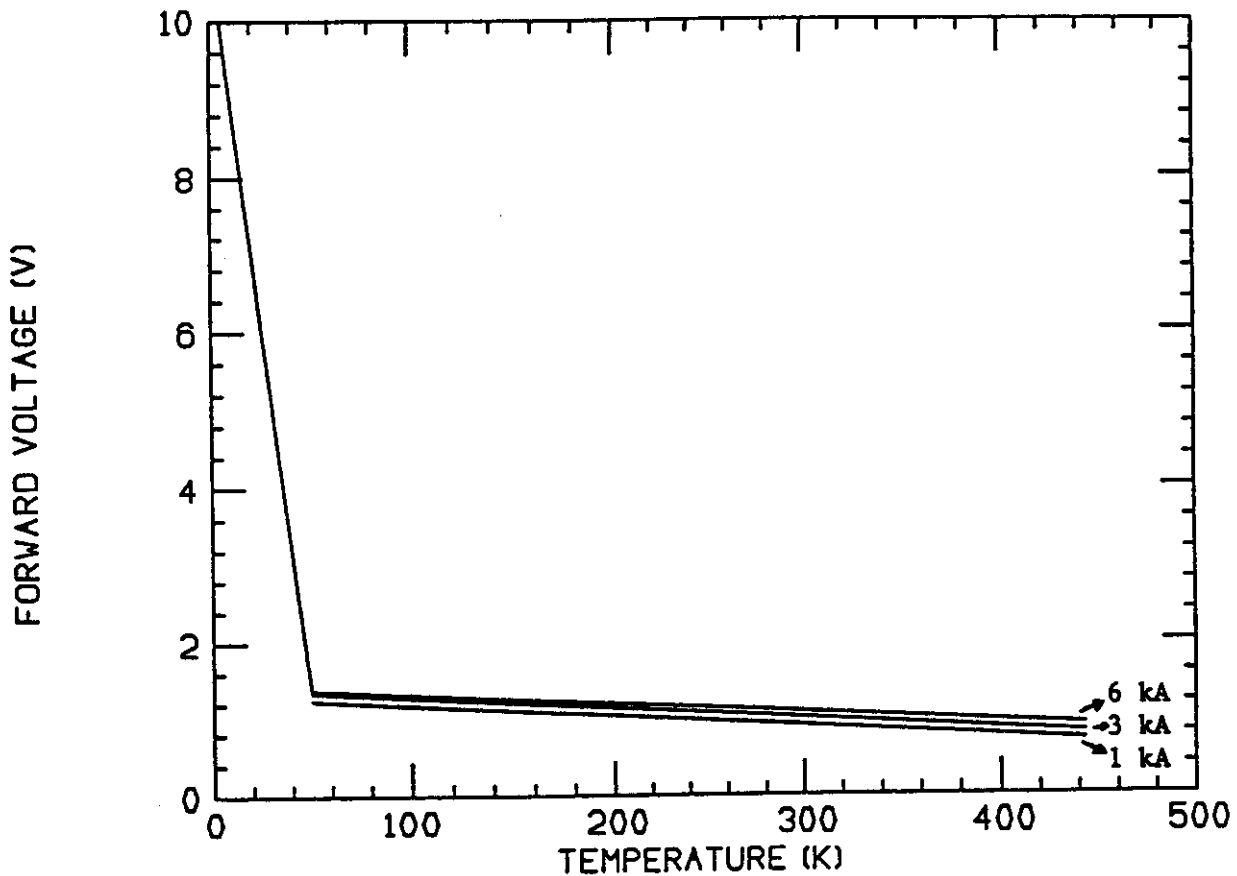


Fig. 12: Approximate DS6000 forward voltage dependence on current and temperature (undamaged diode)

3.5 The SSC quench current pulse

From the CDR /5/, each SSC sector (42 cells of 10 dipoles and 2 quadrupoles each) has a separate power supply, refrigeration system, and quench protection system. The quench protection system consist on the combined action of a slow extraction system and a fast quench bypass system to protect the magnet components. One of the options being considered for the fast bypass system (the passive option) requires cold diodes. In the fast bypass system, after a threshold voltage in the quenched magnet is exceeded, the current is rapidly taken over by the bypass diode, thus protecting quenched the magnet components from excessive power dissipation. This current transfer takes place in approximately 300 ms. Assuming that the magnet was operating at its maximum current, after 300 ms there is going to be a current of 6500 Amps flowing through the bypass diode. After quench detection, the sector power supply voltage is reduced to zero, and the sector magnet current is extracted from the unquenched magnets in the sector by inserting four dump resistors of 0.28 ohms each in series with the magnet power bus (slow extraction system). Since the sector inductance is 22 H, the current will decay exponentially with a time constant of $22/1.22 \sim 20$ sec.

We want to design the heat sink with some safety margin so an irradiated diode can survive the additional heating that results from the failure of one dump resistor to function. In this case, the time constant decay is $22/0.84 \sim 26$ sec. Therefore, the quench current pulse that we considered in our heat sink thermal design has a 300 ms rise time up to 6500 Amps, and then an exponential decay with 26 sec time constant. Fig. 13 shows this current as a function of time.

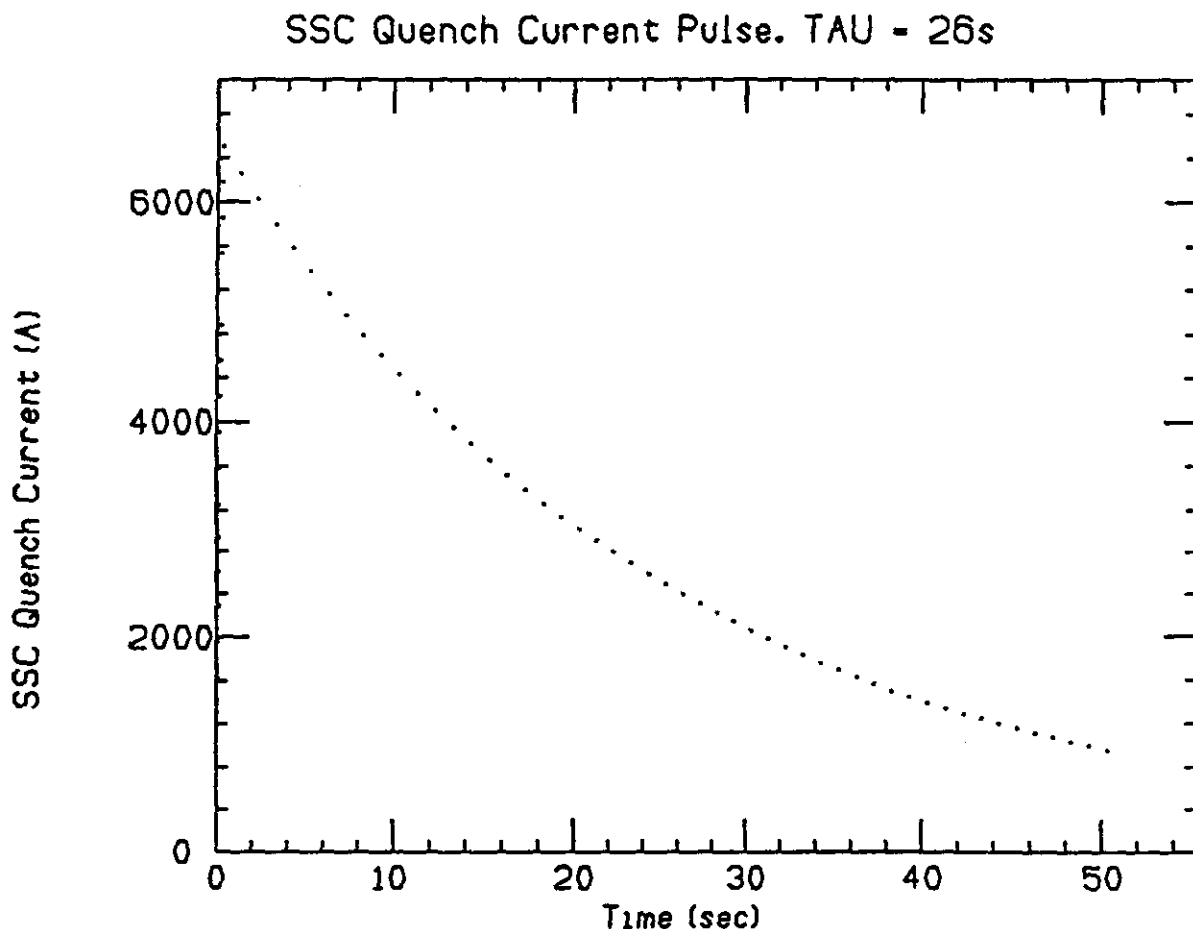


Fig. 13: SSC quench current pulse (at max. current and when one dump resistor fails)

3.6 Approximations

We assumed that the heat sink has adiabatic boundary conditions. This is a conservative assumption, because there is going to be some heat transfer to the environment through power leads, adjacent materials, etc. If the mounting assembling is immersed in Liquid Helium, then we will have to review this assumption because it might be too conservative.

The power dissipated at the junction depends on current, time, and temperature. The standard input of TOPAZ2D accepts functions of either time or temperature, not both. We had to make compromise, so we decided to use an "average" value of VF. One way of doing this is, instead of trying to calculate the average VF, to make a conservative choice, let say, VF at 3000 Amps at 80 K. For example, for an undamaged DS6000 this value is 1.3 V, while at room temperature and 3000 Amps VF is down to 1 V (see Fig. 11). Since most of the time the junction is going to be above 80 K, our choice is conservative.

Another disadvantage of the standard TOPAZ2D input is that it only accepts 8 points to describe the material properties temperature dependence. 8 points are not enough to describe the properties dependence between liquid helium and 450 K, so again we had to make a compromise. If we select an initial temperature of 30 K, we avoid the specification of material properties at very low temperature, where they are very sensitive to temperature (particularly the specific heat). 8 points can be then adequate to describe the properties dependence with temperature in the range 30 K - 450 K. Now, to consider an initial temperature of 30 K instead of 4.35 K is not such a bad assumption because the enthalpy difference of copper is only 0.2 J/g. The energy dissipated by a quench current pulse is about $6500 \times 26 \times 1.3 \sim 220,000$ J, so 2 kg of copper will absorb only 0.2% of this energy when increasing its temperature from 4.35 K to 30 K.

4. RESULTS

After many computer runs, we found that for an SSC quench pulse of 6500 Amps max. with a 26 sec exponential decay constant, the practical maximum average forward voltage drop is 2.3 V. Beyond $VF = 2.3$ V, the maximum junction temperature will exceed its limit of ~ 170 C, no matter how large is the heat sink.

The next step was to optimize the heat sink dimensions for $VF = 2.3$ V. Fig. 14 shows the maximum junction temperature dependence as a function of the heat sink dimensions (radius and length). We selected R (radius) = 5 cm and L (thickness) = 4 cm as optimum dimensions. The slight decrease in maximum junction temperature beyond those values doesn't justify the increase of heat sink volume in our opinion (there is no much room available in the cryostat to place the diodes).

Fig. 15 shows the maximum junction temperature dependence on the average forward voltage for a heat sink of R = 5 cm and L = 4 cm. There is a linear relationship, with a slope of about 175 C/V. For an undamaged diode ($VF \sim 1.3$ V), we predict a maximum junction temperature of about 0 C.

Fig. 16 shows, as a function of time, the junction temperature and the temperature at various distances from the junction for a heat sink with R = 5 cm and L = 4 cm, and for a diode with $VF = 2.3$ V. The maximum junction temperature occurs at about 6 sec from the start of the quench current pulse.

Fig. 17 shows contours of temperature at $t = 6$ sec, the time of maximum junction temperature.

Fig. 18 shows the profile of temperature at the axis ($r = 0$) at $t = 6$ sec. The step-like changes in temperature are due to the presence of contact thermal resistances.

Fig. 19 shows the radial profile of temperature in the diode ($z = 0$) at $t = 6$ sec. The slight decrease of temperature with increasing radius is due to the larger radius of the heat sink, what makes a problem a two-dimensional one. This non-uniform temperature distribution within the diode can have undesirable effects because of the negative temperature coefficient of the diode (current-crowding). This problem needs further investigation.

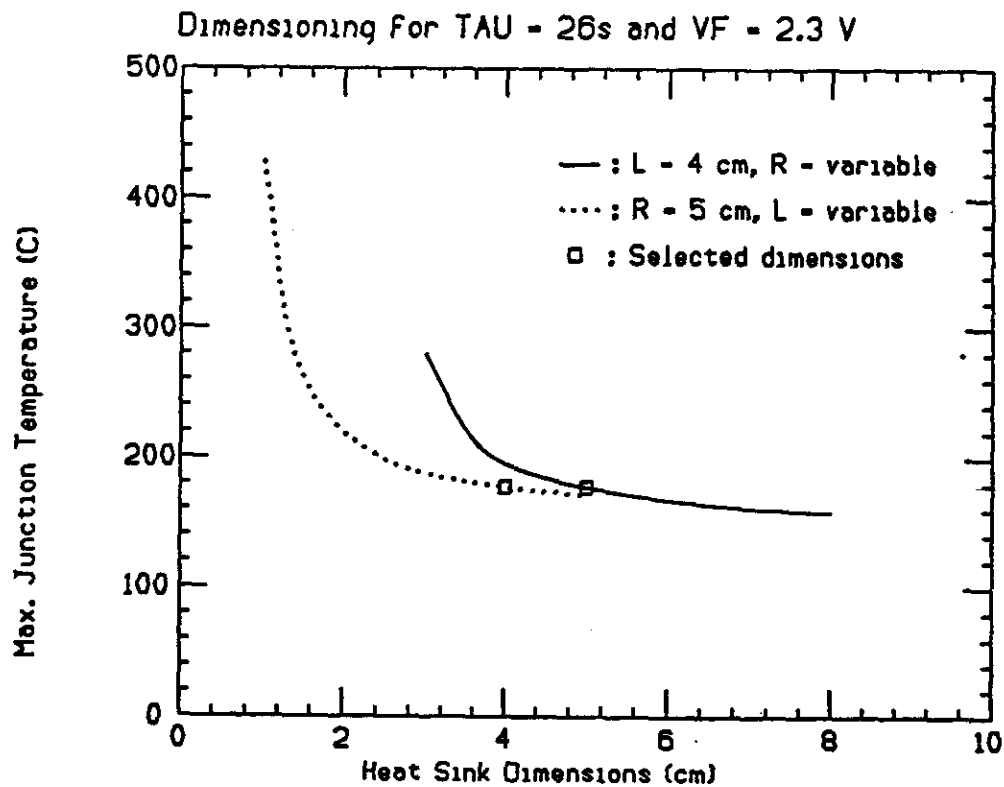


Fig. 14: Maximum Junction temperature dependence on heat sink dimensions for the limit average forward voltage of 2.3 Volts

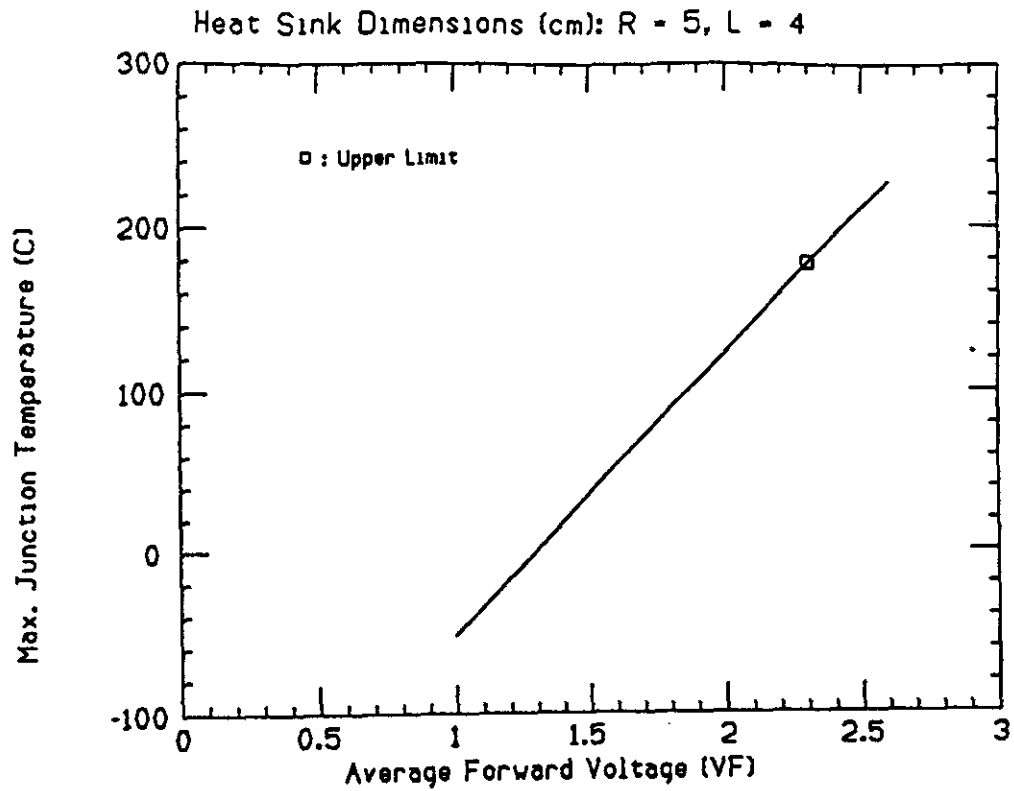


Fig. 15: Maximum Junction temperature dependence on the average forward voltage for the selected heat sink dimensions.

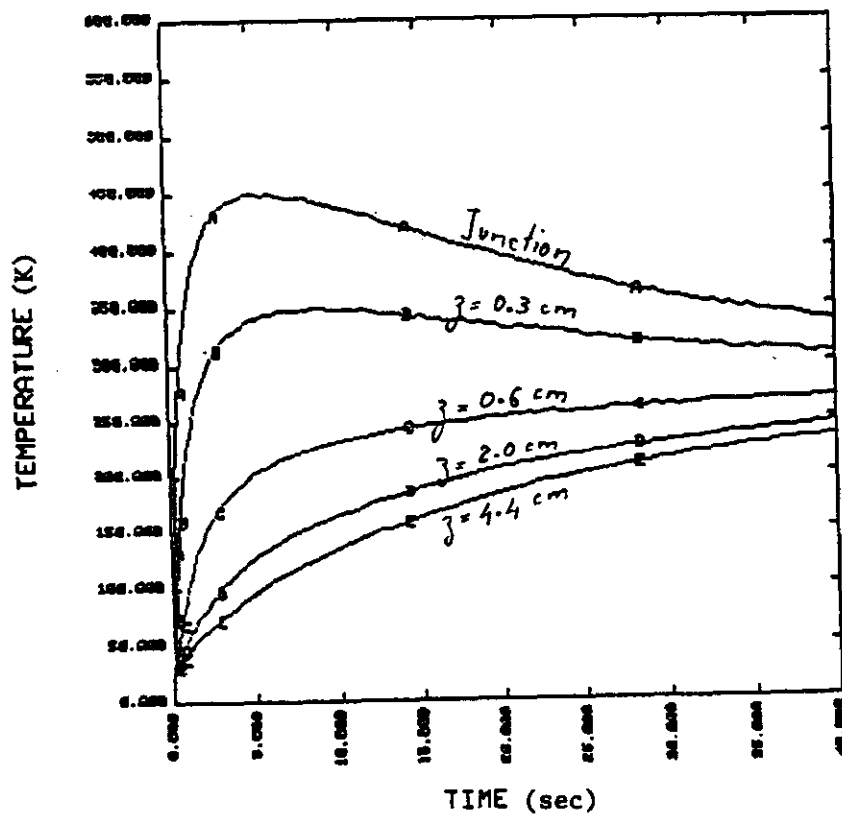


Fig. 16: Temperature at various axial distances from the junction for $V_F = 2.3 \text{ V}$.

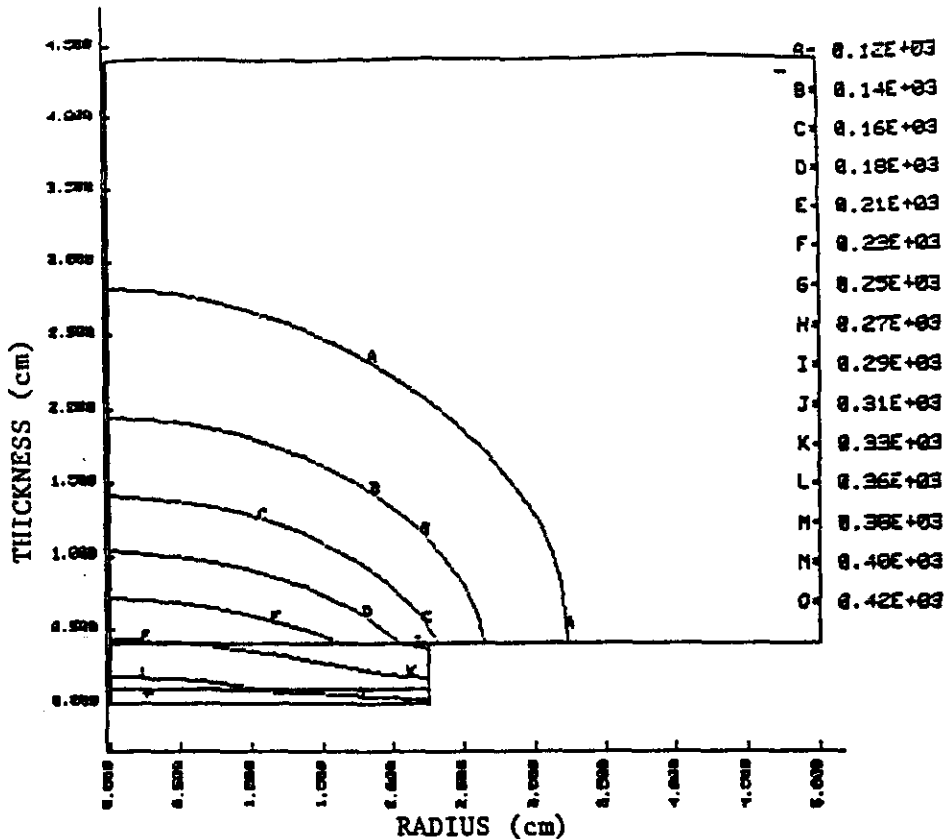


Fig. 17: Contours of temperature at $t = 6$ sec., the time of maximum junction temperature.

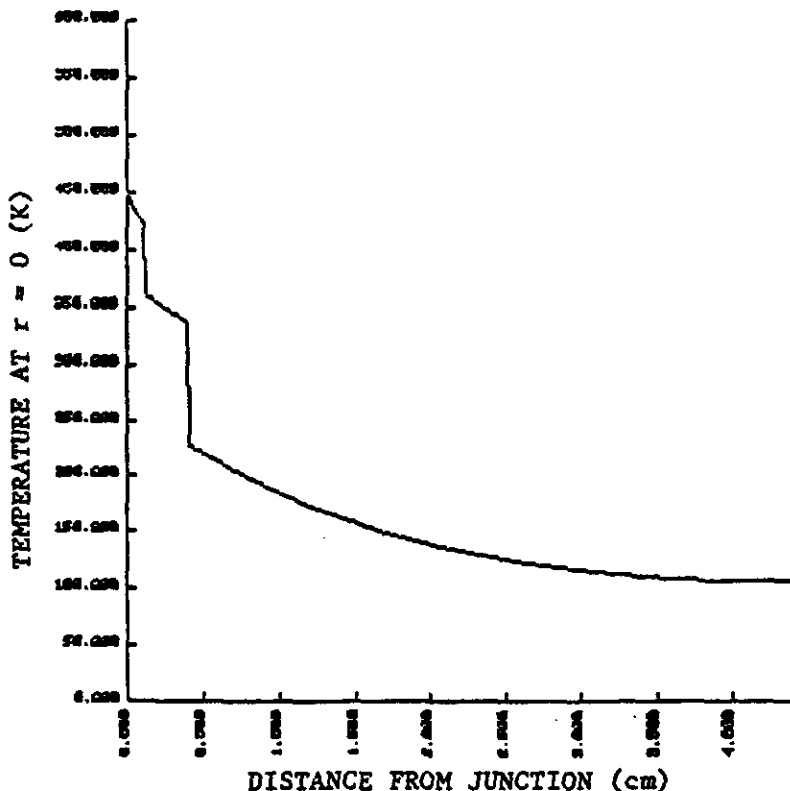


Fig. 18: Profile of temperature at $r = 0$ and $t = 6$ sec, the time of maximum junction temperature.

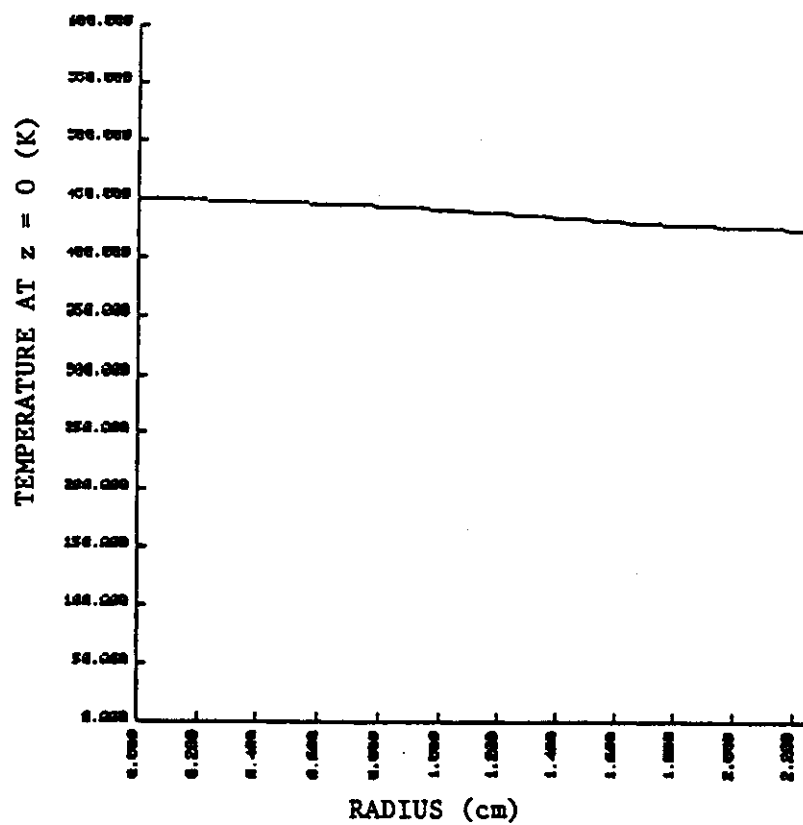


Fig. 19: Radial profile of temperature in the diode ($z = 0$) at $t = 0$ sec, the time of maximum junction temperature.

5. CONCLUSIONS

We have presented a heat sink thermal design for the SSC passive quench protection diodes. The design was based on numerical simulations of the diode junction temperature response under an SSC quench current pulse using the non-linear, time-dependent Finite Element program TOPAZ2D.

The design criteria was to optimize the heat sink dimensions for the "limit" average forward voltage (the maximum average forward voltage for which the maximum junction temperature is 170 C with an infinite heat sink).

As a result of our simulations, we found that the limit average forward voltage is 2.3 V for a copper heat sink, and we proposed an "optimum" heat sink radius of 5 cm and an "optimum" heat sink thickness of 4 cm. With this dimensions, the heat sink design has a safety margin for the failure of one dump resistor.

According to present estimates, the BBC diode DS6000 will have an average forward voltage of 2.3 V after more than 100 years of SSC operation. Therefore, the heat sink will not constitute a limiting factor on the diodes survivability within the SSC lifetime if it has the proposed dimensions. Further studies are under way to narrow the uncertainty of forward voltage increase during SSC operation. In any case, it is important to remember that due to the transient nature of the current pulse, there is not going to be significant changes in the maximum junction temperature nor in the limit average forward voltage for a heat sink with larger dimensions than $R = 5$ cm and $L = 4$ cm.

The heat sink thermal design is a first step toward an overall mounting assembly design; it provides basic dimensions which are necessary for a mechanical design. The next step will include structural analysis (thermal stresses, deformations, etc) to assure a clamping force within specifications during the thermal cycle. Testing of unirradiated and irradiated cold diodes with simulated quench current pulses and reliability analysis are in the end mandatory in order to provide evidence of satisfactory mounting assembly design and in order to assess the impact that the usage of cold diodes has on the availability of the SSC.

6. REFERENCES

/1/ D. Groom, private communication. Also: T. A. Gabriel et al., "Preliminary Simulations of the neutron Flux Levels in the Fermilab Tunnel and Proposed SSC Tunnel", SSC-110, August 1987.

/2/ Specifications for the diode DS6000. BBC Publication No. CH-E 3.40774.2 D/E/F, October 1986.

/3/ J. Zeigler, R. Carcagno and M. Weichold, "Experimental Measurements of Radiation Damage to Power Diodes at Cryogenic Temperatures", presented at the 1987 Particle Accelerator Conference, Washington D.C., March 1987.

/4/ A. B. Shapiro, "TOPAZ2D - A Two-Dimensional Finite Element Code for Heat Transfer Analysis, Electrostatic, and Magnetostatic Problems", LLNL report UCID-20824, July 1986.

/5/ SSC Central Design Group, "Conceptual Design of the Superconducting Super Collider", SSC-SR-2020, March 1986.

7. APPENDIX I: CONTACT THERMAL RESISTANCE

There is a contact thermal resistance (CTR) between the diode package and the mounting assembly. This CTR arises from the fact that under moderate loads the surfaces are in intimate contact only at a number of small discrete spots, and the amount of heat passing through these spots is reduced still further by the "constriction" of the lines of flow /4,5,6,7/. Heat transfer through the interstitial medium can be neglected when we have a vacuum environment of better than 5×10^{-6} torr with boundaries at less than 40 K /4/.

The CTR of an interface across which a temperature drop ∂T exist is defined by:

$$R_c = \frac{\partial T}{Q} \quad (1)$$

where ∂T is in K and Q in Watts.

The macroscopic value of ∂T in (1) has to be understood as the mean value averaged over the interface. Several theoretical models have been developed to account for R_c /4,5,6,7 /; however, most usable data in the field are empirical /1,2,3,4 /.

Previous experimental work in metal-to-metal thermal contact resistance has been done in vacuum as a function of applied contact forces, surface finishing, temperature, and heat flux. The specimen pairs under study were mainly Copper, Stainless-Steel, and Aluminium. It has been concluded that:

- 1) The CTR is independent of the contact area, and depends only on the total load /2/.
- 2) The CTR definitely decreases with the increasing contact force.
- 3) At least in the range 50 - 1000 N a Log(CTR)-Log(Load) linear fit of the experimental data is possible (/1,2/, see Fig. I.1).
- 4) One measurement done at very high load (22,240 N) suggest that a departure from a Log(CTR)-Log(Load) linear relationship must occur at high loads (/2/, see Fig. I.2). The departure tendency is toward lower CTR values than expected, and is presumably related to the destruction of surface layers of oxide. This result could be misleading to our purposes, because the contact geometry was cone-socket instead of rod-rod. We couldn't find any additional measurements at high loads to confirm this departure.
- 4) No correlation could be drawn with respect to surface finishing in the range 0.1 to 1.6 micrometers rms roughness /1/. With few exceptions, it seemed to be that the surface finishing tested are essentially equivalent in terms of CTR.
- 5) In the range 1.6 - 5 K the CTR is approximately proportional to $1/T^2$ in most of the measurements (/1,2/ see Fig. I.2). At Nitrogen temperatures, the temperature dependence is much smaller, changing by only 10% between 65 K and 77 K /2/.
- 6) The $1/T^2$ temperature dependence at helium temperatures is independent of the nature of the junction /2/.
- 7) For Stainless-Steel specimens, the CTR change with temperature in the range 77 K - 300 K is very small (within the measurement error in /4/)

- 8) The CTR at a given temperature and load depends on the temperature at which the contact was made /2/
- 9) It appears that most of the heat transport takes place through electrical insulating regions of the surfaces (surface layers of oxide). At high temperatures, the surface is probably more easily broken than at low temperatures, and the area of metallic contact is greater /2/.
- 10) A large directional effect was reported in /4/. The directional effect refers to a curious property of certain contacts by which they have a greater CTR in one direction across the contact than in the reverse direction. One possible reason for the directional effect is the potential barrier produced by the interfacial oxide layers, which inhibit the electronic heat flux. Work functions are sensitive to the state and preparation of the surfaces, hence there is no reason why a directional effect should not occur between similar materials if the surface histories are different. The directional effect depends upon temperature, load and heat flux for a given specimen pair. Depending on the heat flux direction, 10 to 1000% discrepancy in the measured CTR values for a given contact was reported in /4/. The discrepancy seems to increase with increasing load, decrease with increasing temperature, and decrease with increasing heat flux. The range of temperature measurements in /4/ was 77 K - 300 K, and the specimen pairs tested were mainly Stainless-Steel pairs.
- 11) The CTR doesn't appear to be markedly dependent upon the magnitude of the heat flux, at least at room temperature; a sevenfold increase in heat flux producing not more than 10% CTR change /4/.
- 12) At least at room temperature, a small decrease in CTR with time was noted during a period of 130 hours /4/. It appears that this small decrease is due to the surface hardness time dependence when a constant load is applied /4/.
- 13) The CTR decreases with increasing pressure environment. Fig. I.3 (from /4/) shows this dependence at room temperature.

We can use the previous information together with CTR measurements to estimate the CTR between the diode package and the mounting assembly. The following prevents a direct usage of the measured values for our case:

- The contact force between the diode package and the mounting assembly is 22,240 N, and the contact force in most of the CTR measurements we found are in the range 50 - 1000 N.
- The contact between the diode package and the mounting assembly was made at room temperature and atmospheric pressure. After the contact force was applied, the assembly was placed in a cryostat, vacuum was made, and the assembly was cooled down to liquid helium temperatures. In most of the CTR measurements we found, the contact was also made at room temperature and then cooled down, but the contact was made in vacuum. Perhaps this is an important factor, because if air remains trapped at the interface, then the conclusions are not valid in our case. At this moment, we don't know how to evaluate the existence and/or effect of trapped air on the CTR.
- We couldn't find any intermediate measured values of CTR between liquid helium and liquid nitrogen temperatures nor CTR Copper-to-Copper measurements at room temperature.

We have to make the following assumptions in order to estimate the CTR between the diode package and the mounting assembly:

a. No trapped air at the interface. If this is not the case, the we CTR will be overestimated, because we are neglecting heat transfer through the interstitial medium.

b. An upper bound of the CTR resistance is given by extrapolating linearly the Log(CTR)-Log(Load) dependence at moderate loads to 22,240 N. A lower bound of the CTR resistance is given by reducing the above mentioned extrapolation by a factor of 5. This factor is consistent with the measurement made in /2/ for a Cu cone-Cu socket at 20,906 N and 4.2 K. We assume that the factor is independent of temperature.

c. The CTR $1/T^2$ dependence on temperature is still valid at high loads. This assumption is based on experimental CTR measurements for a Cu cone-Cu socket at 4700 lb /2/.

d. Above 10 K, we assume that the CTR dependence on temperature is proportional to the Copper conductivity dependence on temperature, and we use CTR measured values at liquid nitrogen temperature /2/ as scaling factors. This assumption is not valid at very low temperatures, where we saw that the CTR has a $1/T^2$ dependence no matter what the conductivity dependence on temperature. However, at higher temperatures the metal conductivity dependence on temperature could become dominant, and given the lack of experimental measurements in this range we think that this assumption is not very unreasonable, and at least has some physical support. The weak dependence of the CTR on temperature around Liquid nitrogen temperatures /2/ is in agreement with our conductivity-proportional CTR dependence assumption at high temperatures.

In order to extrapolate CTR measured values to our case, we are going to use the following procedure:

From ref. 1, take measured CTR values in the range 1.6 - 5.6 K for a surface finishing of 1.6 micrometers rms roughness, and for a given temperature make a linear least-squares fit of Log(CTR)-Log(Load) values. Extrapolate the corresponding CTR value for a load of 22,240 N. Repeat the procedure for other temperatures. Then, using the CTR extrapolated values for 22,240 N, make a least-squares fit of CTR- $1/T^2$ values. In this way, we can have the upper bound CTR-temperature dependence at 22,240 N in the range 1.6-5.6 K.

From ref. 2, take measured CTR values at liquid Nitrogen temperatures, make a linear least-square fit of Log(CTR)-Log(Load) values, and extrapolate the corresponding CTR value for a load of 22,240 N. This is the upper bound CTR value at 77 K for a load of 22,240 N.

To obtain the lower CTR-temperature dependence lower bound, reduce the above extrapolated values by a factor of 5.

Between extrapolated measurements, calculate additional points assuming a conductivity-proportional behaviour. Use the CTR extrapolated values at 77 K as scaling factors.

Using the above mentioned procedure, we obtained the curve shown in Fig. 11. We see that the CTR is not negligible, particularly at very low temperatures. The CTR cannot be neglected the thermal model. The combination of low temperatures and vacuum operation results in high values of CTR.

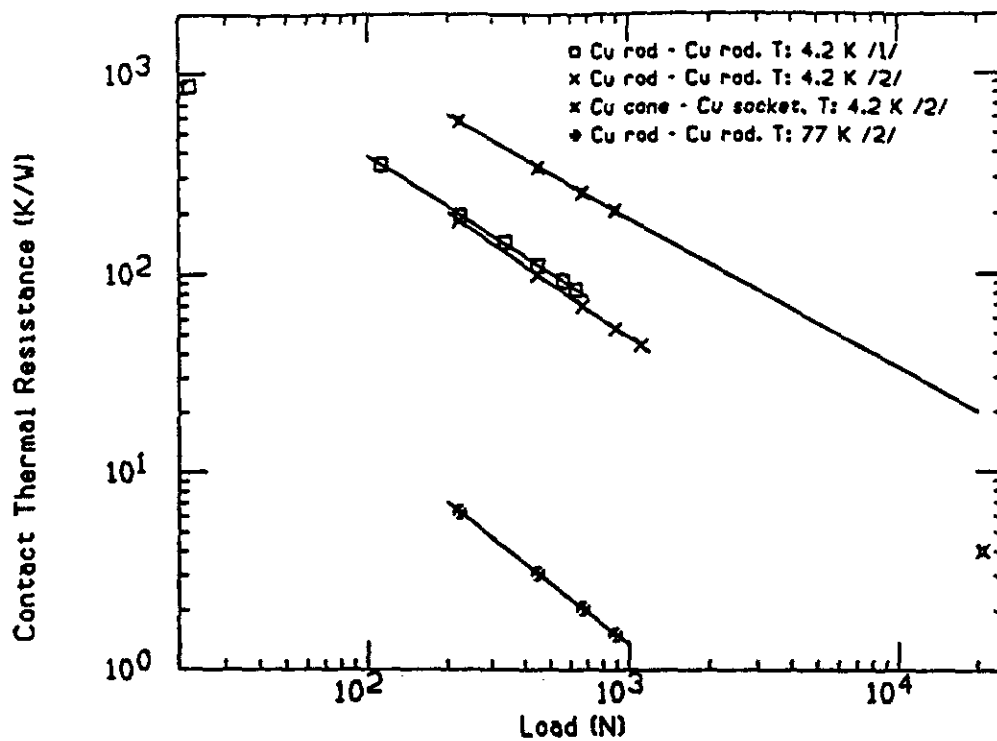


Fig. I.1: Contact Thermal Resistance vs Load

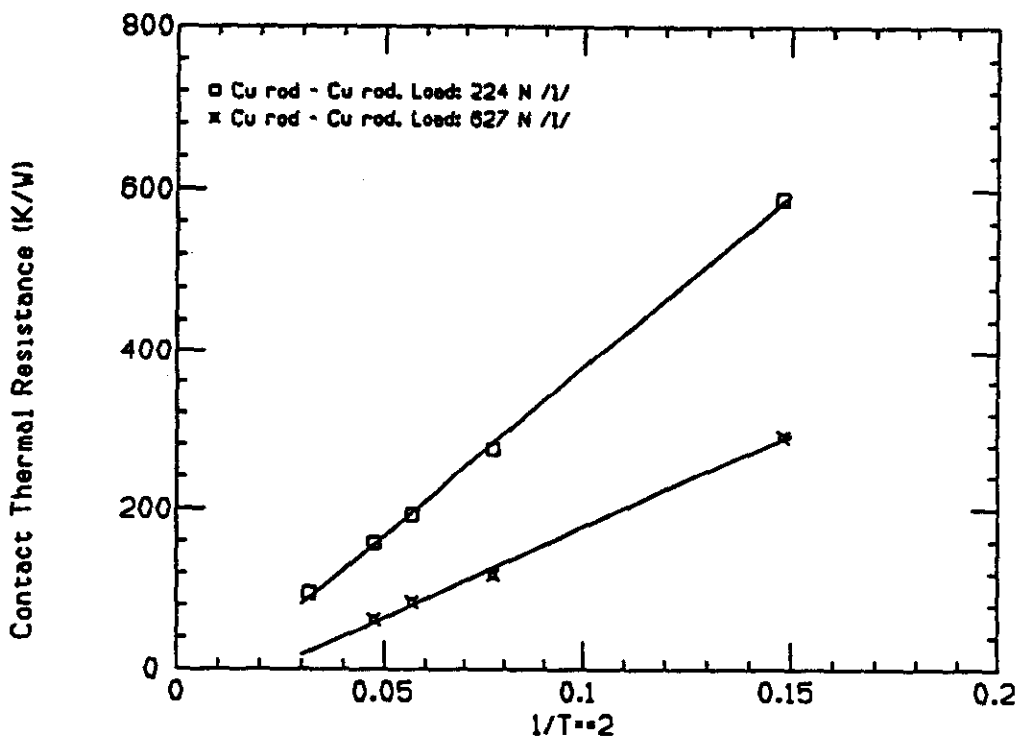
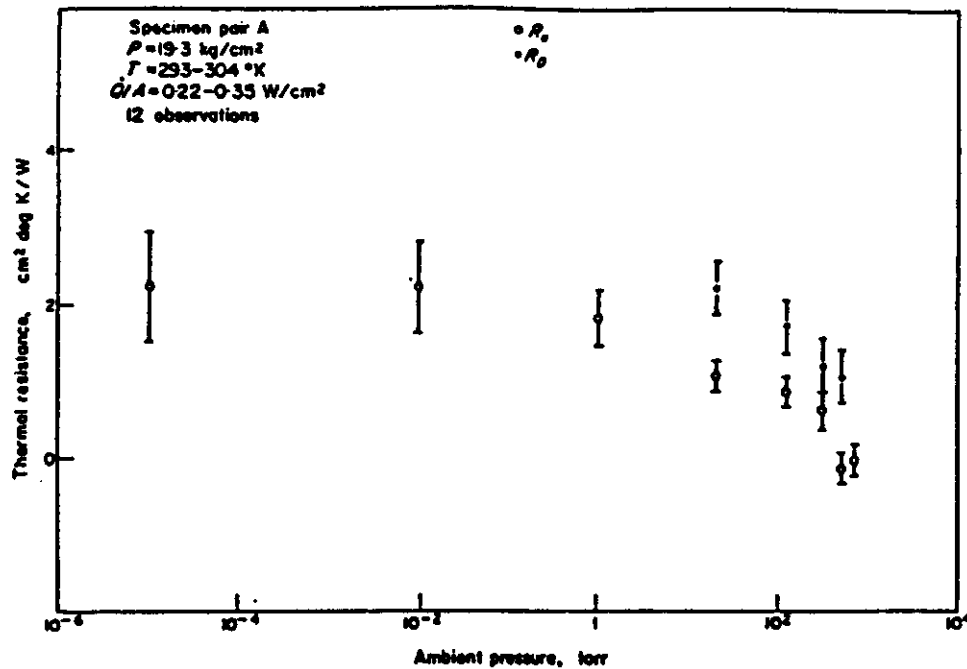


Fig. I.2: Contact Thermal Resistance vs $1/T^2$

THERMAL CONTACT RESISTANCE



Dependence of the contact resistance upon the pressure of the helium environmental gas.

REFERENCES FOR APPENDIX I.

- /1/ L.J. Salerno, P. Kittel and A.L. Spivak, "Thermal Conductance Measurements of Pressed OHFC Copper Contacts at Liquid Helium Temperatures", Thermal Conductivity 18, plenum Press (1985)
- /2/ R. Berman, "Some Experiments on Thermal Contact at Low Temperatures", J. Applied Physics. 27 No 4 (1956)
- /3/ R. Berman and C.F. Mate, "Thermal Contact at Low Temperatures", Nature, Dec. 13 (1958)
- /4/ T.R. Thomas and S.D. Probert, "Thermal Contact Resistance: The Directional Effect and Other Problems", Int. J. Heat Mass Transfer. 13 (1970)
- /5/ M. Bobeth and G. Diener, "Upper Bounds for the Effective Thermal Contact Resistance Between Bodies with Rough Surfaces", Int. J. Heat Mass Transfer. 25, No 8, (1982)
- /6/ M. Bobeth and G. Diener, "Variational Bounds for the Effective Thermal Contact Resistance Between Bodies with Rough Surfaces", Int. J. Heat Mass Transfer. 25, No 1, (1982)
- /7/ M.G. Cooper, B.B. Mikie and M.M. Yovanovich, "Thermal Contact Conductance", Int. J. Heat Mass Transfer. 12, (1969)